Coherence of rainfall propagation as simulated in the WRF model using two different convective schemes

ANDREW J. ANSORGE
Meteorology Program, Iowa State University, Ames, IA

Mentors: Adam J. Clark[1] and James Correia Jr.[2]
Department of Geological and Atmospheric Sciences, Iowa State University, Ames, IA[1]
Department of Agronomy, Iowa State University, Ames, IA[2]

ABSTRACT

Numerical Weather Prediction (NWP) models continue to make advances and improvements to weather forecasts; however, convective precipitation remains poorly forecasted in mesoscale models. This study examines two convective schemes and whether one performs better in mostly strongly forced cases over a two-month period where convective propagating precipitation occurred. Observations were compared to precipitation forecasts generated by the Weather Research and Forecasting model using the Betts-Miller-Janjic and Kain-Fristch convective schemes. Propagation speed and beginning longitude were measured by using Hovmöller diagrams for both convective schemes and observations. Results show that the KF was closer to observations in propagation speed and beginning longitude compared to the BMJ. Examination of the diurnal averaged Hovmöller diagrams revealed that the BMJ convective precipitation was significantly less than the KF.

1. Introduction

Prediction of convective precipitation poses continued challenges for Numerical Weather Prediction (NWP) models (Olson et al. 1995). A recent study suggests that precipitation episodes demonstrate coherent propagating rainfall patterns over the central United States, which indicates intrinsic predictability of convective systems (Carbone et al. 2002). If forecast models could accurately depict convective propagating precipitation events by using the innate predictability, then the prediction of warm-season rainfall may improve in models.

However, further investigation revealed that models could not produce coherent rainfall patterns (Davis et al. 2003). The cumulus parameterization schemes are the main challenge to poor model performance as they tend to trigger precipitation too early and propagate precipitation too slowly (Davis et al. 2003). Additional proof that convective schemes are responsible for poor model performance was shown in a study by Liu et al. (2006; herein L06) using a coarse resolution version of the Pennsylvania State University-National Center for Atmospheric Research Mesoscale Model Version 5 (MM5; Dudhia 1993) using a convective scheme to a high-resolution version of the MM5 model without a convective scheme. Results indicated that the high-resolution model without the convective scheme simulated propagating precipitation episodes better than the low-resolution MM5 (Liu et al. 2006). In addition, L06 concluded that models simulating propagating precipitation episodes using the Betts-Miller (BM; Betts and Miller 1993) convective scheme do better than those using the Kain-Fritsch (KF; Kain and Fritsch 1993 and Kain 2004) scheme in frequency and location over a small-time period.

The BM and Betts-Miller-Janjic (BMJ; Betts 1986; Betts and Miller 1986; Janjic 1994) were developed for large-scale models, which may be a disadvantage if the BM and BMJ are used in fine-resolution runs of the Weather Research and Forecasting (WRF; Skamarock et al. 2001; Michalakes et al. 2001) model. However, both the BMJ and KF miss propagating nighttime precipitation with the KF having more difficulties than the BMJ (Liu et al. 2006).

KF falsely produced precipitation over the eastern and southern boundaries of the domain, produced precipitation over a too widespread of an area and predicted rainfall areas propagating too slowly (Liu et al. 2006). In addition, L06 found the KF produces precipitation too far north and is too widespread in its placement of precipitation compared in both weak and moderate large-scale forcing cases. However, the BMJ tends to overpredict light precipitation (Jankov and Gallus 2004). Errors in the cumulus parameterization have made mesoscale models inaccurate in predicting warm-season propagating precipitation episodes. Furthermore, even when mesoscale models were predicting a precipitation streak, the model did not initiate the precipitation at the right time (Davis et al. 2003).

While the BMJ and KF convective scheme both produce convective precipitation, there are some key differences between these cumulus parameterization schemes to be discussed. Both the BMJ and KF adjust temperature and specific humidity. BM removes the conditional instability by fitting a moist reference adiabatic profile. This scheme activates when there is an abundance of low to mid-level moisture with a significant amount of positive convective available potential energy (CAPE), but does not take into account vertical velocities directly. The KF rearranges the mass in a vertical column to eliminate CAPE. The trigger function for the KF is grid-resolved upward vertical motions (Gallus et al. 1999).

This study aims to reexamine the findings of L06 that the BMJ simulates convective propagating precipitation episodes better than the KF. WRF simulations using 15-km grid-spacing centered over the Midwest will be examined using the BMJ and KF convective schemes to compute statistics of the beginning longitude, propagation speed and start time of the precipitation events. These quantities will be compared to observations.

My hypothesis is that the BMJ will perform better than the KF in producing precipitation at the beginning longitude and have similar propagation speeds when compared to observations. The time period chosen consists mostly of strongly forced cases where fronts are associated with convective precipitation (Carbone et al. 2002). Thus, strong surface convergence may be found in these strongly forced cases, which will lead the KF scheme to activate more often than the BMJ (Jankov and Gallus 2004). Therefore, the KF should overpredict and produce the precipitation over a wider area whereas the BMJ will be closer to the observed precipitation in amount and placement. The BMJ may give results closer to observations because it uses thermodynamics and is constrained by the amount of moisture in a grid-column (Baldwin et al. 2002).

The paper is arranged as follows: Data and methodology for this study is in section

2, results in section 3, and a summary and conclusion in the final section.

2. Data and methodology

Rainfall forecasts were generated at Iowa State University using the WRF model (Version 2.1.1) with the Advanced Research WRF (ARW) dynamic core over a domain from $104°$ to $88°$W (eastern Colorado to western Indiana) and from $35°$ to $50°$N (central Oklahoma to the Canadian border). Grid spacing was 15km and forecast length was 120 hours. Precipitation was output every 3 hours. The time period chosen was an active two-month period from 26 March – 22 May 2006 of mostly strongly forced cases. The model was initialized at 0000Z with initial conditions (IC) and lateral boundary conditions (LBC) obtained from the Global Forecast System (GFS) model (Environmental Modeling Center 2003). Ferrier et al. (2002) microphysics and Mellor-Yamada-Janjic (Mellor and Yamada 1982; Janjic 2002) planetary boundary layer parameterization were used. WRF-ARW forecasts were verified using 3-h accumulated precipitation from NCEP Stage-IV multi-sensor analyses (Baldwin and Mitchell 1997). Both the day 1 (forecast hours 0-24) and day 2 (forecast hours 24-48) forecasts were used to see differences in the modeled forecasts.

a. *Convective precipitation*

To determine if precipitation was convective, national radar composites with severe thunderstorm and tornado watch boxes overlaid from the Iowa Environmental Mesonet (IEM) were used (Fig. 1). If there was a watch located within the domain, precipitation was counted as convective as long as there was precipitation associated in or near the watch box that supported the watch box (e.g. tornado watch box and light precipitation was not considered convective). To

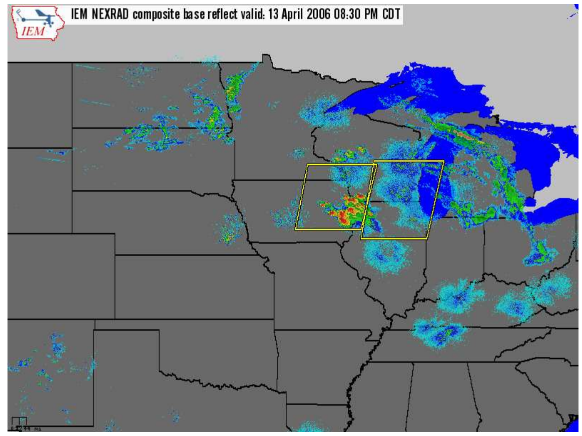

FIG. 1: National radar composite with watch boxes overlaid valid 13 April 2006 at 0130Z from the IEM. This day featured an outbreak of late afternoon severe weather including the Iowa City tornadoes.

determine if the precipitation was propagating, the IEM's national radar composite was again used to ensure that precipitation was indeed progressing from west to east. There were several cases of cutoff lows where precipitation either was in a band that formed east to west, but moved north. This was not considered propagating precipitation. With the cutoff lows, there was also precipitation that moved westward. Technically, westward movement could be used for propagation; however, westward propagation is not considered a propagating precipitation episode in this study.

b. *Propagation speeds*

To calculate convective precipitation propagation speeds, time-longitude, or Hovmöller diagrams, similar to Carbone et al. (2002), are used as shown in Fig. 2. If the precipitation was determined to be convective using the above method, propagation speed was calculated in m/s along with the longitude at which convective precipitation was initiated (beginning longitude) and the start time. This was accomplished by beginning at our mini-

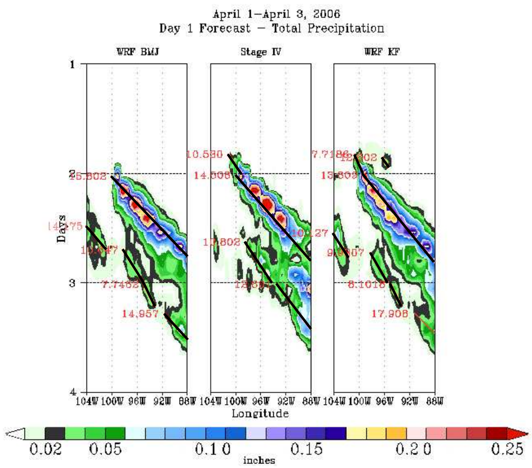

Fig. 2: Example of calculating propagation speed, beginning longitude, and start time of precipitation in Hovmöller space for the episode 1 April - 3 April 2006 for BMJ, KF, and Stage IV total precipitation.

mum threshold of 0.02 inches and proceeding through the center of the precipitation streak, which must contain a relative maximum of 0.03 inches or greater. Propagation ends when our minimum threshold is met, at the edge of our domain, or at the end of a day. An exception to this method occurred when there was precipitation that fit the above criteria, but was spatially separated. If it could be determined that this spatially separated precipitation was one episode, then it was calculated as such; if not, propagation was not calculated.

c. *Number of precipitation events*

After narrowing down the data by only plotting convective and propagating precipitation events, further restrictions are applied. There were several occurrences of the model forecasting precipitation, but the observations did not have the event. The same is true where the observations show an event, yet the model does not forecast the event. Therefore, only precipitation events that occurred both in the model and the forecast were plotted and analyzed (Table 1 and 2). It should also be noted that events that occurred in the BMJ might not be the identical event to the KF and vice versa. This is not a direct comparison of events, but rather an assessment of predicted event statistics.

Total	Observed	Not Observed
Forecast	32/34	5/7
Not Forecast	22/20	21/20
Convective	Observed	Not Observed
Forecast	9/29	0/5
Not Forecast	42/24	25/21

Table 1: Contingency table for total and convective precipitation day 1 forecasts where the first number is the number of BMJ convective propagating precipitation events and the second is the number of KF events (BMJ/KF).

Total	Observed	Not Observed
Forecast	28/29	8/11
Not Forecast	11/10	25/24
Convective	Observed	Not Observed
Forecast	7/28	0/10
Not Forecast	32/12	30/25

Table 2: Same as Table 1, except number of convective propagting precipition events for day 2 forecast.

3. Results

Convective, non-convective and total precipitation were compared to observations for both the day 1 and day 2 forecast. Non-convective precipitation will not be discussed, except in the diurnal cycle, as total precipitation includes non-convective precipitation. The discussion below is broken down into convective and total precipitation for day 1 and day 2 forecasts followed by a brief examination of the diurnal cycle, which is illustrated by Hovmöller diagrams of average precipitation at each forecast hour for the entire period analyzed.

a. *Convective precipitation*

The BMJ convective precipitation has two to three times fewer events than the KF in both day 1 and day 2 forecast (Table 1 and 2). The scarce number of events in the BMJ is further seen when we compare the BMJ to the KF in beginning longitude and propagation speed as all of the BMJ events occurred in the first 0-12 or 24-36-h forecasts (Fig. 3). While the majority of KF's events are in the 0-12-h forecast, there is a trend to more of a balance in the day 2 forecast with about an even number of events for both the 24-36 and 36-48-h forecast (Fig. 4).

When comparing Figs. 3 and 4, the BMJ's 0-12-h forecast is close to the 1-1 line indicating that observations were in line with the model whereas the 24-36-h is placed further east in longitude. However, the KF 0-12 and 24-36-h forecasts are close to the observa-

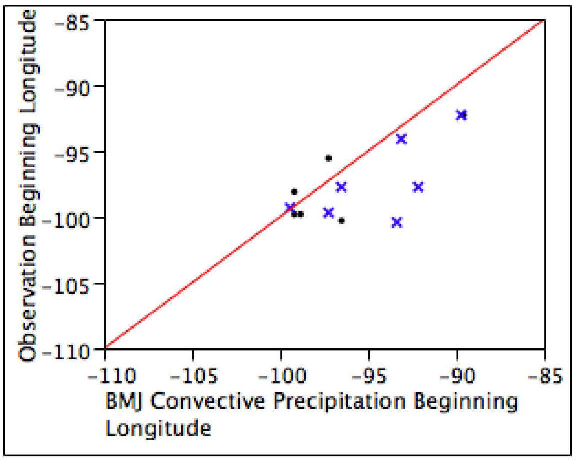

FIG. 3: BMJ convective precipitation beginning longitude. A dot is the 0-12-h forecast, + is the 12-24-h forecast, x is the 24-36-h forecast and a box is the 36-48-h forecast.

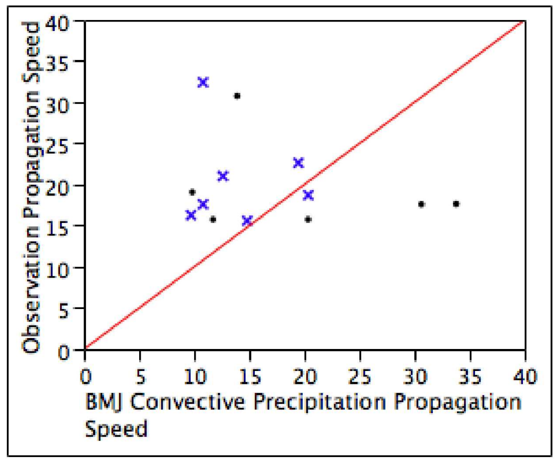

FIG. 5: Same as Fig. 3, except for BMJ convective precipitation propagation speed in m/s.

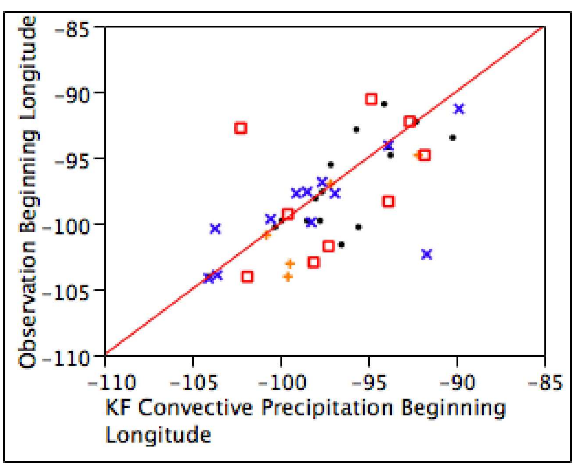

FIG. 4: Same as Fig. 3, except for KF convective precipitation beginning longitude.

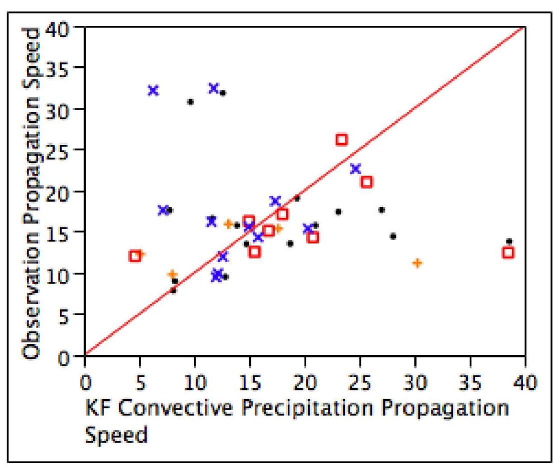

FIG. 6: Same as Fig. 3, except for KF convective precipitation propagation speed in m/s.

tions. The KF 12-24 and 36-48-h forecasts show beginning longitude further east of observations.

The BMJ's 0-12-h forecast reveal that while observations were fairly similar in events, the BMJ had a spread of speeds (Fig. 5). The 24-36-h forecasts present slower propagation speeds in the BMJ model. KF is closer to observations than the BMJ in all forecast hours (Fig. 6). Overall, KF's propagation speed and beginning longitude were better than the BMJ's when compared to observations.

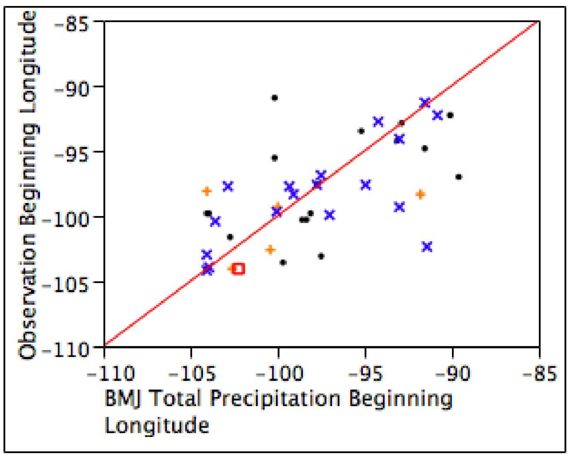

FIG. 7: KF total precipitation beginning longitude. A dot is the 0-12-h forecast, + is the 12-24-h forecast, x is the 24-36-h forecast and a box is the 36-48-h forecast.

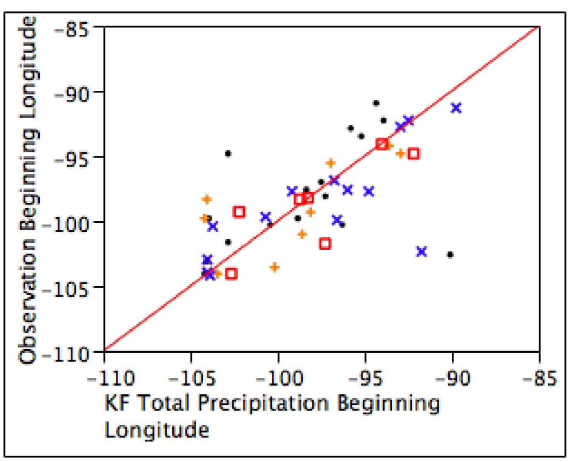

FIG. 8: Same as Fig. 7, except KF total precipitation beginning longitude.

b. *Total precipitation*

While the number of events becomes more balanced in the total precipitation, the KF continues to perform better than the BMJ. The BMJ does produce precipitation events in the 12-24 and 36-48-h forecasts unlike the convective precipitation. The KF has fewer events overall in the same timeframe whereas the convective precipitation had an equal number of events in the each 12-h forecast.

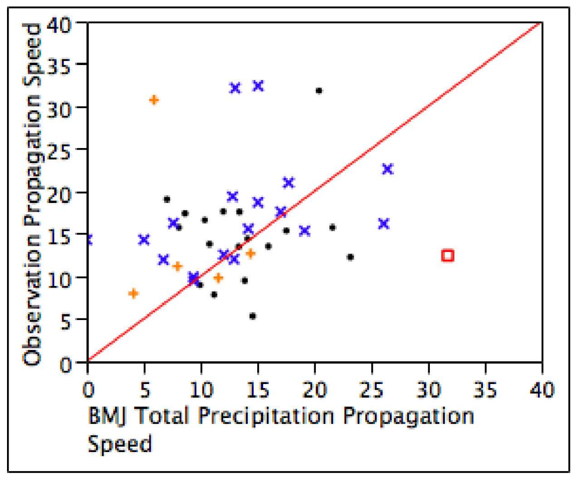

FIG. 9: Same as Fig. 7, except BMJ total precipitation propagation speed in m/s.

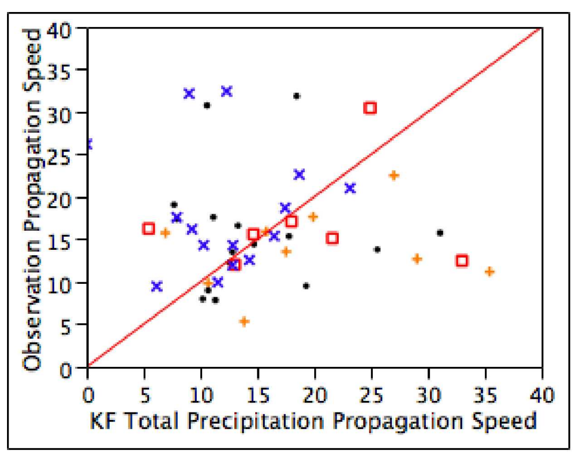

FIG. 10: Same as Fig. 7, except KF total precipitation propagation speed in m/s.

The BMJ tends to slightly begin precipitation further to the east in longitude in all of the forecast hours (Fig. 7). The KF shows results in the 0-24-h forecasts were better than the 24-48-h forecasts when compared to observations (Fig. 8). However, the 0-24-h forecast from the KF exhibited a bias to place precipitation slightly to the west of observations whereas the 24-48-h forecast had a tendency to place precipitation further to the east of observations.

Propagation speed for the BMJ was best in forecast hours 0-12 and 24-36, but all forecast hours propagated precipitation slower than observations (Fig. 9). When compared to the KF, the 0-12 and 24-36-h forecast produced propagation speeds that were faster than the observations, but closer to the observations than BMJ (Fig. 10). The 12-24 and 36-48-h forecast also was closer to observations than the BMJ, but was instead slower compared to observations. As stated in the convective precipitation, BMJ is inferior to the KF.

c. *Diurnal cycle*

It is shown that the BMJ non-convective scheme produces more precipitation than the convective scheme with the largest latitudinally averaged amount from the convective scheme being less than three tenths (Fig. 11). The KF, however, produces more precipitation in the convective precipitation, but the non-convective precipitation also has a fair amount of precipitation and is more balanced between convective and non-convective precipitation than the BMJ (Fig. 12). It should be noted that there are well-defined propagating precipitation streaks in the observations and the KF total precipitation whereas in the BMJ, these streaks are less coherent (Fig. 13). There is a tendency, especially further out in forecast hours, to begin propagating precipitation further east of the observations in the convective and total precipitation for both the BMJ and KF.

4. Summary and conclusions

A two-month period of mostly strongly forced cases was studied to see if the BMJ or KF convective scheme would perform closer to the observations. Hovmöller diagrams were used to calculate propagation speed, beginning longitude and start time, which then were compared to the observed data for day 1 and day 2 forecasts.

While precipitation was shown to be propagating, the hypothesis that the BMJ would perform better than the KF as found in L06 was shown to be false in strongly forced cases. The KF had more precipitation events, which were more in line with observations. Thus, the convective and total precipitation was best represented in the KF. For longitude and propagation speed, KF was closer to observations, especially the 0-12 and the 24-36-h forecast.

The diurnal cycle showed that the BMJ's precipitation is driven by the non-convective scheme whereas the KF favors the convective scheme in precipitation amount. Precipitation streaks were evident in the observations, but only the KF total and convective precipitation exhibited these streaks. The BMJ produced precipitation over a widespread area and did not yield propagating streaks.

While the KF did perform closer to observations, in both the BMJ and KF convective and total precipitation, the beginning longitude generally had a bias to begin propagating precipitation east of observations. While forecast days 3-5 were not studied, it was shown that the beginning longitude continues to be placed further to the east of the observation.

The key results are as follows:

- The KF total precipitation beginning longitude 0-12-h forecast placed precipitation west of observations while the 24-36-h forecast placed precipitation further to the east of observations.

- There were more precipitation events in the KF than in the BMJ, especially in the convective scheme.
- The KF propagation speeds were closer to the observations than the BMJ.
- BMJ non-convective precipitation produces more precipitation than the convective scheme.
- BMJ propagation speeds were slower compared to observations.

Acknowledgments. Grid Analysis and Display System (GrADS) was used to calculate propagation speed and the propagation's beginning longitude and start time. Thanks to Adam Clark for providing the data and software support and Jon Hobbs for statistical assistance.

5. References

Baldwin, M.E., J. S. Kain, and M. P. Kay, 2002: Properties of the Convection Scheme in NCEP's Eta Model that Affect Forecast Sounding Interpretation. *Wea. Forecasting*, **17,** 1063-1079.

——, and K. E. Mitchell, 1997: The NCEP hourly multisensor U. S. precipitation analysis for operations and GCIP research. Preprints, *13th Conf. On Hydrology,* Long Beach, CA, Amer. Meteor. Soc., 54-55.

Betts, A. K., 1986: A new convective adjustment scheme. Part 1: Observational and theoretical basis. *Quart J. Roy. Mteor. Soc.*, **112,** 677-692.

——, and M. J. Miller, 1986: A new convective adjustment scheme. Part II: Single column tests using GATE wave, BOMEX, and arctic air-mass data sets. *Quart J. Roy. Mteor. Soc.*, **112,** 693-709.

——, and ——, 1993: The Betts-Miller scheme. The representation of cumulus convection in numerical models. *Meteor. Monogr.,* **46,** 107-121.

Carbone, R. E., J. D. Tuttle, D. A. Ahijevych, and S. B. Trier, 2002: Inferences of predictability associated with warm season precipitation episodes. *J. Atmos. Sci.,* **59,** 2033-2056.

Davis, C. A., K. W. Manning, R. E. Carbone, S. B. Trier, and J. D. Tuttle, 2003: Coherence of warm-season continental rainfall in numerical weather prediction models. *Mon. Wea. Rev.,* **131,** 2667-2679.

Dudhia, J., 1993: A nonhydrostatic version of the Penn StateNCAR Mesoscale Model: Validation tests and simulation of an Atlantic cyclone and cold front. *Mon. Wea. Rev.,* **121,** 14931513.

Environmental Modeling Center, 2003: The GFS atmospheric model. Technical Procedure Bulletin No. 442, NCEP/NWS.

Ferrier, B. S., Y. Jin, Y. Lin, T. Black, E. Rogers, and G. DiMego, 2002: Implementation of a new grid-scale cloud and precipitation scheme in the NCEP Eta model, Preprints, *15th Conf. On Numerical Weather Prediction, San Antonia, TX, Amer. Meteor. Soc.,* 280-283.

Gallus, W. A., Jr., 1999: Eta simulations of three extreme precipitation events: sensitivity to resolution and convective parameterization. *Wea. Forecasting*, **14,** 405-426.

Janjic, Z. I., 1994: The step-mountain Eta coordinate model: Further development of the convection, viscous sublayer, and turbulence closure schemes. *Mon. Wea. Rev.,* **122,** 928-945.

——, 2002: Nonsingular implementation of the Mellor-Yamada Level 2.5 Scheme in the NCEP Meso Model. NCEP Office Note No. 437, 61 pp.

Jankov, I., and W. A. Gallus, Jr., 2004: MCS rainfall forecast accuracy as a function of large-scale forcing. *Wea. Forecasting*, **19,** 428-439.

Kain, J. S., and J. M. Fritsch, 1993: Convective parameterization for mesoscale models: The Kain-Fritsch scheme. The representation of cumulus convection in numerical models. *Meteor. Monogr.,* **46,** 165-170.

——, 2004: The Kain-Fritsch Convective Parameterization: An Update. *J. Appl. Meteor.,* **43,** 170-181.

Liu, C., M. W. Moncrieff, J. D. Tuttle, and R. E. Carbone, 2006: Explicit and parameterized episodes of warm-season precipitation over the continental United States. *Advances in Atmospheric Sciences,* **23,** 91-105.

Mellor, G. L., and T. Yamada, 1982: Development of a turbulence closure model for geophysical fluid problems. *Rev. Geophys. Space Phys.,* **20,** 851-875.

Michalakes, J., S. Chen, J. Dudhia, L. Hart, J. Klemp, J. Middlecoff, and W. Skamarock, 2001: Development of a next generation regional Weather Research and Forecast Model. *Developments in Teracomputing: Proceedings of the Ninth ECMWF Workshop on the Use of High Performance Computing in Meteorology*, W. Zwieflhofer and N. Kreitz, Eds., World Scientific, 269-276.

Olsen, D. A., N. W. Junker, and B. Korty, 1995: Evaluation of 33 years of quantitative precipitation forecasting at the NMC. *Wea. Forecasting*, **10,** 498-511.

Skamarock , W. C., J. B. Klemp, and J. Dudhia, 2001: Prototypes for the WRF (Weather Research and Forecasting) Model. Preprints, *Ninth Conf. on Mesoscale Processes*, Fort Lauderdale, FL, Amer. Meteor. Soc., J11-J15.

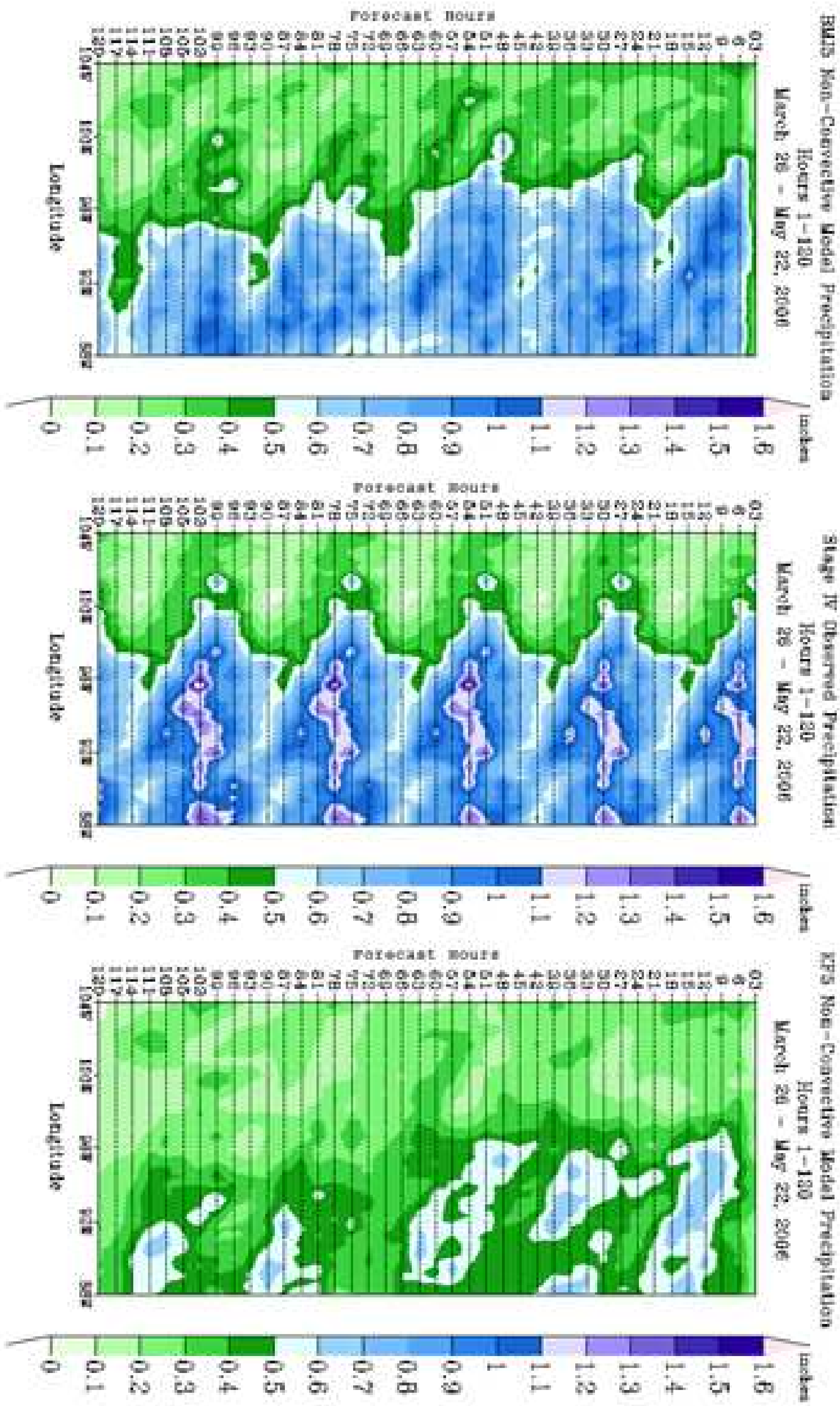

Fig. 11: BMJ non-convective precipitation (left), observations (center), and KF non-convective precipitation (right) for the forecast hours 0-120 (days 1-5) depicting the diurnal cycle.

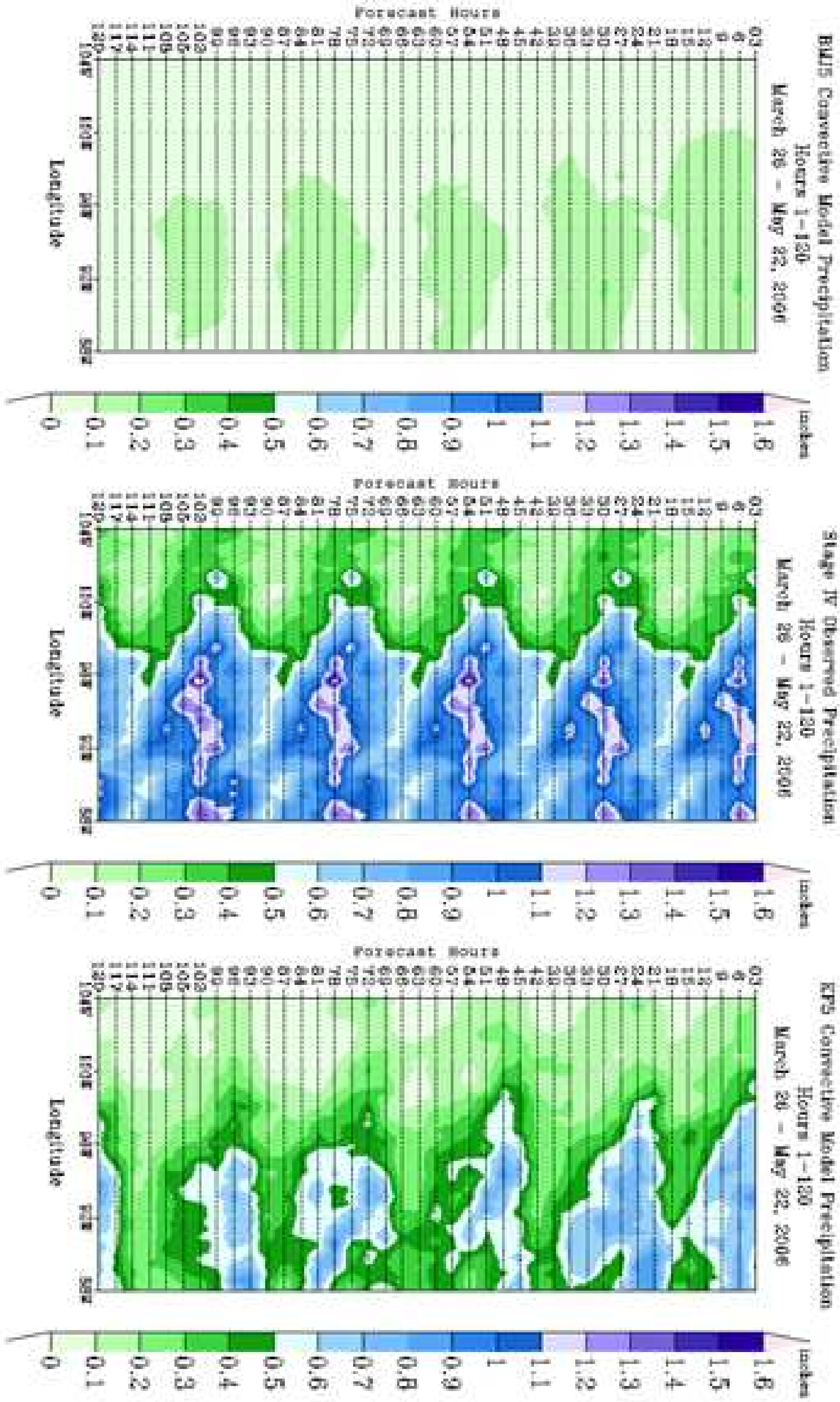

Fɪɢ. 12: Same as Fig. 11, except for convective precipitation.

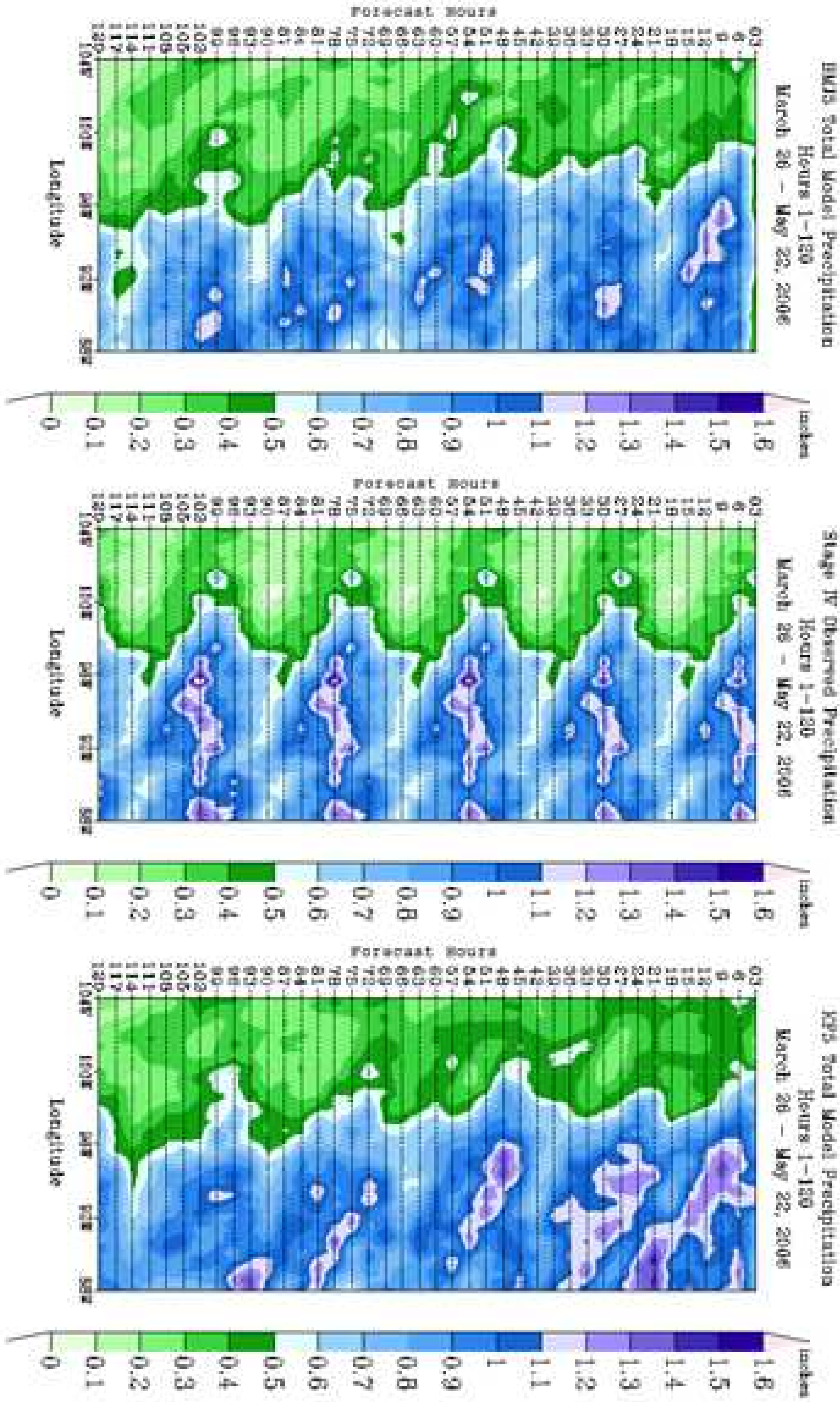

Fig. 13: Same as Fig. 11, except for total precipitation.